HAL
open science

Sulfamethazine degradation by heterogeneous photocatalysis with ZnO immobilized on a glass plate using the heat attachment method and its impact on the biodegradability

Taous Aissani, Idris Yahiaoui, Farouk Boudrahem, Lamia Yahia Cherif, Florence Fourcade, Abdeltif Amrane, Farida Aissani-Benissad

To cite this version:

Taous Aissani, Idris Yahiaoui, Farouk Boudrahem, Lamia Yahia Cherif, Florence Fourcade, et al.. Sulfamethazine degradation by heterogeneous photocatalysis with ZnO immobilized on a glass plate using the heat attachment method and its impact on the biodegradability. Reaction kinetics, mechanisms and catalysis, 2020, 131 (1), pp.471-487. 10.1007/s11144-020-01842-4 . hal-02957715

HAL Id: hal-02957715

https://hal.science/hal-02957715v1

Submitted on 16 Nov 2020

HAL is a multi-disciplinary open access archive for the deposit and dissemination of scientific research documents, whether they are published or not. The documents may come from teaching and research institutions in France or abroad, or from public or private research centers.

L'archive ouverte pluridisciplinaire **HAL**, est destinée au dépôt et à la diffusion de documents scientifiques de niveau recherche, publiés ou non, émanant des établissements d'enseignement et de recherche français ou étrangers, des laboratoires publics ou privés.

Sulfamethazine degradation by heterogeneous photocatalysis with ZnO immobilized on glass plate using heat attachment method and its impact on the biodegradability

Taous Aissani[1], Idris Yahiaoui[1], Farouk Boudrahem[1], Lamia Yahia Cherif[1], Florence Fourcad[2], Abdeltif Amrane[2] Farida Aissani-Benissad[1]

(1) Laboratoire de Génie de l'Environnement (LGE), Faculté de Technologie, Université de Bejaia, 06000, Alegria.
(2) Univ Rennes, Ecole Nationale Supérieure de Chimie de Rennes, CNRS, ISCR (Institut des Sciences Chimiques de Rennes) – UMR 6226, F-35000 Rennes, France
E-mail : Taous.aissani@outlook.fr.
tel. 00 (213)34215704

Abstract

In this paper, the degradation of sulfamethazine (SMT) was performed using of photocatalytic process in the presence of ZnO catalyst immobilized on glass plate (on ZnO/glass plate) under UV light. The ZnO/glass plate was characterized by X-ray diffraction (XRD) and Fourier transform infrared (FTIR) spectra; the results of the characterization demonstrated that the properties of ZnO/glass plate were maintained unmodified. The adsorption and the photolysis tests revealed the absence of adsorption of SMT onto ZnO/glass plate and the absence of direct photolysis of SMT. The effect of the initial solution pH, the flow rate and the initial concentration of SMT on the photocatalytic process was studied and optimized by using central composite design (CCD). The model equation obtained led to a classification of these parameters based on their level of significance. The results suggested that the most influential factor was the initial concentration of SMT (x_2), which had the strongest effect on the response (-11.6) and the negative sign of the coefficient suggested that the degradation of SMT decreased for increasing initial SMT concentration. It was followed by the flow rate with positive effect on the yield of SMT degradation (+2.06). The model also demonstrated the absence of pH effect in the studied interval and that the strongest interaction was between the pH and the flow rate. The kinetic of degradation of the SMT can be described by a pseudo

Accepted Manuscript

first order kinetic model for 10 and 50 mg/L of SMT; while the kinetic of degradation was described by a pseudo-second-order kinetic model for the highest initial amount, $[SMT]_0$=100 mg/L. The optimal values of the solution pH, the flow rate and the initial concentration of SMT were 6, 0.56 L/min and 11 mg/L respectively. Under these conditions the removal efficiency of SMT was 96 % and the BOD_5/COD ratio increased from 0 to 0.20 after 5h of irradiation time.

Keywords: Photocatalytic process, Sulfamethazine, immobilized ZnO, Central composite design

Accepted Manuscript

1. Introduction

Pharmaceuticals are being continuously released into the aquatic environment through different anthropogenic activities [1]. In particular, antibiotics can cause ecotoxicological problems, because of their potential persistence in the environment [2], since they are not readily biodegradable. Consequently, they are detected in surface water and groundwater; several pharmaceuticals have been detected in the μg L^{-1} range in wastewaters [3]. For sulfamethazine (SMT), Concentrations in the range 15-328 $ng.l^{-1}$ were detected in tropical waters in the Mekong Delta, Vietnam [4]. In China, comparable concentrations of SMT were observed in natural waters, e.g, 0.53–89.1 ng L^{-1} in surface water of the Yangtze estuary [5] and 2.05-623.27 ng L^{-1} in the Huangpu River, Shanghai [6]. Such diffuse pollution is difficult to treat, and hence one solution would be to treat the considered pollution on site, to get low volumes highly concentrated [7]. For this purpose, several processes to degrade/remove antibiotics have been studied, including conventional techniques (biological processes, filtration, coagulation, flocculation, and sedimentation), advanced oxidation processes (AOPs), adsorption, membrane processes, and combined methods [8]. The advanced oxidation processes (AOP_S) appears as interesting tools in comparison with other technique [9]. They are based on the generation of very reactive species such as hydroxyl radicals, that have been proposed to oxidize quickly and not selectively a broad range of organic pollutants[10,11]. Among AOPs, photocatalysis using viz., TiO_2 and ZnO, appears effective for the pharmaceutical wastewater treatment. Photocatalytic conversion using ZnO showed better degradation efficiency than TiO_2 for removing organic compounds from water [12-14]. The technique is more effective as compared to other AOPs because semiconductors are inexpensive and can easily mineralize various organic compounds [15]. Among different conventional catalysts, ZnO nanoparticles have been widely used to treat wastewater because of wide band gap, large volume-area ratio, low cost, large initial rate of activities and UV

Accepted Manuscript

adsorption potential [16]. However, the elimination of ZnO suspended in the treated water causes running costs and induces secondary pollution, which greatly restricts its practical applications. Consequently, several methods have been implemented to immobilize ZnO nanoparticles on various substrates, such as activated carbon [17], carbon black (CB)/ZnO nanocomposite film [16], polystyrene pellets [18], glass substrates [19], L-Cysteine capped zinc oxide nanoparticles were immobilized onto a biodegradable poly(3-hydroxybutyrate-co-3-hydroxyhexanoate) [20]. Maučec et al. immobilized ZnO nanoparticles in mesoporous silica supports [21]. These techniques must meet the following conditions: i) Strong adherence between the catalysts and the substrate, ii) The Crystal structure of the catalysts must be kept during the preparation and the immobilization process, iii) low cost of the substrate and the used method [22-27].

Physicochemical methods such as flocculation–coagulation, adsorption, have been widely investigated. However, The removal of dyes and recalcitrant pollutants from wastewater using these methods was not as effective as expected; in addition, most of these methods are nondestructive, since they only consist in a transfer of organic compounds from water to another phase, thus causing secondary pollution [28-32]. For the degradation of persistent organic compounds contained in wastewater, several studies recommend integrated processes, especially the coupling of AOPs and biological treatment [28-34]. The main objectives of this study are: i) to use a heat attachment method to immobilize ZnO on glass plate (9 cm × 35 cm). This material was of soda-lime type, soda-lime glass is inexpensive and chemically stable, such immobilization method remains scarcely investigated in this research area; ii) to use the experimental design methodology to investigate the influence of the main experimental parameters (flow rate (Q_v), the pH and the initial SMT concentration) on the efficiency of the photocatalytic degradation of SMT with ZnO immobilized on glass plate in batch reactor, iii) to examine the feasibility of combining UV/ZnO process with biological

Accepted Manuscript

treatment to eliminate the SMT from aqueous solutions, such combination has not been extensively examined in the available literature.

2. Materials and methods

2.1. Chemicals and photocatalytic system

The SMT ($C_{12}H_{14}N_4O_2$, 99% purity) from Alfa Aesar, sulfuric acid (96 % purity) and sodium hydroxide (97 % purity) both from Biochem Chemopharma. Zinc oxide (99 % purity) from Sigma Aldrich and hydrofluoric acid (HF) (40%) were purchased from prolabo (Paris, France). The Experimental setup is described in the supplementary material (See Fig.1). It is composed of a Vessel (1) fitted with a Pyrex glass jacket (2) connected to a thermostated bath (3) in order to maintain the solution at a temperature of 25°C and a stirrer in stainless steel (4) was used for the homogenization. A glass plate loaded with ZnO (5), one UV lamp (6) (30 W,UVA, λ_{max} = 360 nm, manufactured by Philips, Netherlands), a centrifugal pump (7) which allows to circulate the solution through the plate, and an air pump (8) was used to provide the solution with dissolved oxygen required for the experiment. 1 L of SMT solution was placed into the reactor; its pH was adjusted by adding concentrated solutions of H_2SO_4 or NaOH. Experiments were monitored for 5 h at a temperature of 25°C. Samples of 5 mL were withdrawn at regular time intervals for the measurement of the SMT residual concentrations.

2.2. Immobilization of ZnO on glass plates

ZnO nanoparticles were fixed on glass plate (9 cm×35 cm) by heat attachment method; the glass surface was pretreated with HF solution (0.1 M) and then washed in a solution of NaOH (0.01M) in order to increase the number of OH groups and ensure a good fixing of the ZnO on the glass plate. Twenty millilitres (20 mL) of suspension containing 4 g/L ZnO were prepared using ethanol as solvent and the suspension was stirred magnetically for 2 h times. The suspension was poured into a glass plate and then placed in a drying oven at 30°C. After

Accepted Manuscript

drying, the plates were calcined at 500°C for 1h and the surface was then washed with distilled water for the removal of weakly attached ZnO [28]. Under the effect of heat the particles became welded together, forming the cohesion [28].

2.3. Characterization

The X-ray diffraction (XRD) patterns of ZnO nanoparticles powder, glass plate and ZnO immobilized on glass plate were obtained using a diffractometer panalytical type MPD/system vertical θ/θ, using radiation source (CuKα = 0.15406 nm) operating at 40 kV and 30 mA. The XRD diffraction patterns were collected over a 2θ range located between 10° and 80° using an incremental step size of 0.02° with 6 s of acquisition time per step. In addition, the band gap was estimated by means of UV–vis diffuse reflectance spectra (DRS) and by UV-Vis Spectroscopy (Shimadzu, UV-2600). Fourier transform infrared (FTIR) transmission spectra of ZnO nanoparticles powder and ZnO immobilized on glass plate were obtained on an IR Affinity-1 Shimadzu FTIR spectrometer. FTIR analysis was done by scraping the ZnO deposit on the glass plate then KBr Pellet method was applied to form the FTIR spectra. All FTIR spectra were obtained using an FTIR spectrometer over the wavenumber range of 400 and 4000 cm^{-1}.

2.4. Sulfamethazine analysis

SMT was analyzed by High Performance Liquid Chromatography (HPLC ACC 3000 HPLC). The HPLC was equipped with a standard degasser, an autosampler and a pump (Model LPG 3400 SD), as well as a detector with visible ultraviolet ray (UV/ Vis detector VWD 3400 RS). The separation was achieved on a Thermo Fisher scientific (Germany) C18 (5 mm; 4.6 ×150 mm) reversed-phase column. The mobile phase consisted of acetonitrile/ultrapure water (35/65 v/v) with a flow rate of 0.5 mL min^{-1} and the detection of sulfamethazine was carried out at 268 nm.

2.5. COD and BOD_5 measurements

All COD and BOD_5 measurements were duplicated. Chemical oxygen demand (COD) was measured by means of Kits Nanocolor® 15–160 mg/L. COD according to DIN ISO 15705 at

Accepted Manuscript

148°C. The amount of oxygen required for the oxidation of the organic and mineral matter at 148 °C for 2 h was quantified after oxidation with $K_2Cr_2O_7$ at acidic pH and under heating. The BOD_5 measurements were carried out in Oxitop IS6 (WTW, Alès, France). Activated sludge from a wastewater treatment plant (Sidi Ali Labhar, Béjaia- Algeria) was used to inoculate the flasks; the initial microbial concentration was 0.5 g L^{-1}. More details about BOD_5 measurement with Oxitop IS6 (WTW, Alès, France) can be found in a previous study [29].

2.6. Zn^{2+} measurements

The concentrations of Zn^{2+} ions was determined by using SCHIMADZU AA6500 atomic absorption spectrophotometer (SAA) connected to the microcomputer; the analysis was conducted with an oxidizing air-acetylene at 213.8 nm [29].

2.7. Response Surface Methodology (RSM)

Statistically designed experiments based on a RSM were conducted to study the combined effects and the optimization of the flow rate (Q_V), the pH, and the initial SMT concentration. The combinations of the model performance was described using a second-order polynomial equation (Eq. 1) based on a central composite design (CCD). More details about the construction of the CCD model can be found in previous papers [35-37].

$$\hat{y} = b_0 + \sum_{i=1}^{3} b_i x_i + \sum_{i=1}^{3} b_{ii} x_i^2 + \sum_{i=1}^{3} \sum_{j=i+1}^{3} b_{ij} x_i x_j \qquad (1)$$

Where:

- Predicted yield ($\hat{y}$)
- the coefficients of the response model ($b_1, b_2, ..., b_n$)
- linear terms, corresponding to the variables ($x_1, x_2, ..., x_n$)
- squared terms, corresponding to the variables ($x^2_1, x^2_2, ..., x^2_n$)

Accepted Manuscript

- first-order interaction terms for each paired combination (x_1x_2, x_1x_3,...,$x_{n-1}x_n$)

The response was expressed as the percent of yield abatement of SMT (Eq.2):

$$y(\%) = \frac{[SMT]_0 - [SMT]_t}{[SMT]_0} 100 \quad (2)$$

Where $[SMT]_0$ and $[SMT]_t$ were *SMT* values of sample at the initial time 0 and at a given time *t* (mg L^{-1}), respectively.

The original values of each factor and their corresponding levels are shown in the supplementary material (Table 1).

3. Results and discussion

3.1. Characterization studies

- ZnO immobilized on glass plate was characterized by X-ray diffraction (XRD), acccording to the figure 2 given in supplementary material the following conclusion can be drawn: The results shown in Fig. 2 indicate that the glass plate without ZnO nanoparticles presented some amorphous peaks in the XRD curve. The XRD patterns of ZnO nanoparticles powder shows that no diffraction peaks of other impurities were detected. The ZnO nanoparticles diffraction peak appeared in the XRD pattern of ZnO immobilized on glass plate; indicating that the process of dispersion in glass plate did not have an influence on the crystal form of the commercial ZnO nanoparticles powder corresponding to a wurtzite phase, characteristic of the commercial ZnO nanoparticles powder [38]. The figure 3 in supplementary material shows the band gap of the ZnO powder (a) and ZnO immobilized on glass plate (b). According to Figure 3 (see supplementary material) there is no change in the bandgap potential of the semiconductor after immobilization.

Accepted Manuscript

- FTIR spectra of ZnO powder (**a**) and ZnO immobilized on glass plate (**b**) are displayed in the figure 4 given in supplementary material. In the spectrum (**a**), the band at 500 cm^{-1} was assigned to the Zn–O. In addition, a weak band can also be perceived in the range of 3550-3450 cm^{-1}, attributed to the stretching of the O–H, which could be localized on the surface of the catalyst. It should be observed that the characteristic bands of ZnO were maintained in the spectra of ZnO immobilized in the glass plate.

.

3.2. Effect of the amount of catalyst

The effect of the amount of ZnO immobilized on glass plate was investigated for 50 and 100 mg/L of SMT. The amount of ZnO was varied in the range from 0.08 to 0.24 g, corresponding to one to three ZnO deposits. As can be seen in figure 1, the increase of the amount of ZnO immobilized on glass plate from 0.08 to 0.16g promoted the removal efficiency of SMT from 76 to 83 % and from 42 to 65 % after 300 min of reaction time for 50 and 100mg/L of SMT respectively. While, increasing the amount of ZnO from 0.16 to 0.24g did not increase significantly the removal efficiency of SMT, namely 2% regardless of the initial concentration of SMT. Consequently, two layers of ZnO (0.16 g) was selected as the optimal value of the amount of catalyst**.**

Fig. 1

3.3. Adsorption and photolysis tests

Preliminary experiments were performed to assess the adsorption capacity in the dark of ZnO immobilized on glass plat at pH = 6, T = 25°C, Q_v=0.52 L/min, 0.16 g of ZnO and 50mg/L of SMT. According to the figure 5 given in supplementary material, an absence of adsorption of SMT onto ZnO immobilized on glass plate was observed, this results could be attributed to the absence of electronic attraction between SMT and the catalyst. Indeed, the SMT presents a

Accepted Manuscript

neutral form for pH values in the range 2.5 to 7.5 and the point of zero charge (pH_{pzc}) of ZnO is 8.6 [39, 40]. The photolysis of SMT was studied for an initial SMT concentration of 50 mg/L in the absence of ZnO for 60 min. As shown in figure 5 (see supplementary material), direct photolysis did not cause any degradation of SMT.

3.4. Regeneration of the photocatalyst

To study the stability of ZnO immobilized on the glass plate, at the end of a cycle, the glass plate was washed with distilled water in order to remove the SMT and by-products formed during the previous experiment and adsorbed on the catalyst. The degradation efficiency is shown in figure 2, showing a decrease in the removal efficiency of SMT from 84.5 to only 70 % after six cycles. It was probably due to the accumulation of by-products on the surface of catalyst.

Fig. 2

3.5. Modeling and optimization

3.5.1. Elaboration and analysis of the model

The results of the second-order models are presented in the supplementary material (Table 2). The coefficients of polynomial model were calculated by a standard least-square regression method using "Excel" software. Three tests were required to evaluate the adequacy of the model: the Student's t test, which was used to determine the significant coefficients, discarding the insignificant ones, the R^2 test and the Fisher test. All these statistical tests were previously described in details [35-37].

According to these results, the coefficients of the polynomial model can be expressed by the following equation:

Accepted Manuscript

$$y = 74.59 - 11.6x_2 - 2.73x_1x_3 + 2.06x_3^2 \quad (3)$$

According to the regression equation (Eq.3), the initial concentration of SMT (x_2) had the strongest effect on the response (-11.6) and the negative sign of the b_2 coefficient suggests that the degradation of SMT decreased for increasing initial SMT concentration. Kinetic study confirmed this tendency as can be seen in figure 3. According to the figure 3, The results obtained indicate that the degradation efficiency of SMT was inversely proportional to its initial concentration; this may be attributed to a competitive consumption of the hydroxyl radicals between the SMT molecules and the generated by-products, or the decrease of generated h^+ holes and/or $^{\bullet}OH$ radicals at the catalyst surface since the active sites are occupied by the pollutant, or by a decrease of the intensity of the radiation absorbed by the catalyst due to the molecules of the pollutant [3,8,41,42]. The same tendency was previously reported by Kheniche et al. [41] and Andronic et al. [42].

Fig. 3

The second significant factor was the flow rate (x_3) with positive effect on the yield of SMT degradation (+ 2.06). In order to confirm this effect, kinetic experiments were conducted (Figure 4) at different flow rates (0.15 - 0.68 L/min). The results showed that when the flow rates was increased from 0.15 to 0.52 L/min, the SMT degradation over 300 min of reaction time increased from 74 % to 85%. Contrarily, beyond 0.52 L/min the yield of the SMT degradation decreased from 85% to 81% for 0.68 L/min flow rate. To better explain the relationship between the degradation rate and the flow rate, it was considered necessary to

Accepted Manuscript

determine the value of the film thickness of the liquid which can be calculated by the following equation [43]:

$$Thickness\ film = \left(\frac{\Gamma^2}{g}\right)^{1/3} \quad (4)$$

Where: $\Gamma = \frac{Q}{L}$ is the flow rate per unit length (m^3/s m), L is the length of the glass plate, Q is the flow rate (m^3/s) and g the gravity (m/s²).

According to the table 1, the thickness of the liquid film increased with increasing of the flow rate, The decrease in the rate of degradation beyond 0.52 L/min flow rate may be attributed to the limitation of the UV-light penetration on account of the rise of the liquid thickness, in agreement with other reports, Yahia cherif et al [28] and Zayani et al [44], and to the decrease of the residence time in the reactor. The decrease in the rate of degradation of SMT for decreasing flow rates (Q_v = 0.15) can be consequently attributed to the fact that the residence time rose, favoring the surface reactions; this may be also due to the degradation of by-products adsorbed on the surface of the catalyst.

Fig. 4

Table 1

The solution pH did not have significant effect on the yield of SMT degradation, which was confirmed by the time-courses (Figure 5a). On the other hand, pH time-courses were also displayed in figure 5b. The pH increased until being close to pH 5 for acidic initial pH = 3 and decreased from 9 to 7 in the alkaline medium. This effect was attributed to the ZnO dissolution and the formation of Zn^{2+} [45, 46], which can be attributed to the oxidation of ZnO by h^+_{VB} according to the equation 5. Daneshvar et al [45] reported that the photocorrosion of ZnO is complete at pH lower than 4, while no photocorrosion of ZnO takes

Accepted Manuscript

place at pH higher than 10. The ZnO photocorrosion in an acidic medium and alkaline medium were given by Eqs. (6) and (7). In this study, the concentration of Zn^{2+} ions were 17.9, 6.5, and 4.1 mg/ L for pH solution values of 3, 6, and 9 respectively.

$$ZnO + 2h_{B_V}^{+} \rightarrow Zn^{2+} + O^{\cdot} \quad (5)$$

$$ZnO + 2H^{+} \rightarrow Zn^{2+} + H_2O \quad (6)$$

$$ZnO + H_2O + 2OH^{-} \rightarrow Zn^{2+} + H_2O \quad (7)$$

Fig. 5

The model also underlined that the strongest interaction was between the solution pH (x_1) and the flow rate (x_3); this interaction is illustrated in the supplementary material (see the figure 6).

3.5.2. Kinetic studies

In this study, the First-order, Second-order and Langmuir-Hinshelwood (L-H) (see table 3 in in the supplementary material) were tested in order to determine the kinetic model of SMT degradation. A nonlinear method was used in order to optimize the different constants of the models (see supplementary materiel) by minimizing the error function using the solver add-in with Microsoft's spreadsheet, Microsoft Excel. The error function employed (Eq. (8)) was as follows (Aissani et al. [29] and Boudrahem et al. [47]).

$$D(\%) = \sum_{i=1}^{p} \left(\left| \frac{C}{C_0} \right|_{Exp} - \left| \frac{C}{C_0} \right|_{Cal} \right)^2 \quad (8)$$

Where $\left|\frac{C}{C_0}\right|_{Exp}$ and $\left|\frac{C}{C_0}\right|_{Cal}$ are the experimental and calculated data, respectively, and P is the number of experimental data.

Accepted Manuscript

The results given in the figure 6 and the table 2 show that for low concentrations (10 and 50 mg/L), the kinetic was described by a pseudo-first order kinetic model. However, for 100 mg/L of SMT the kinetic was described by a pseudo-second order kinetic model. The absence of adsorption in dark of SMT onto ZnO immobilized on glass plate and the kinetic degradation of SMT was non described by Langmuir-Hinshelwood model confirm that the photocatalytic degradation of SMT does not take place on the surface of the catalyst but in the close vicinity of the catalyst surface [29, 48].

Fig. 6

Table 2

3.5.3. Optimization of the operating variables

The model equation (Eq. 3) obtained by the CCD was used to find the optimal values of the operating parameters in order to obtain the highest degradation rate of SMT. Response surface and contour plot were drawn using STATISTICA software (Figure 7 in supplementary material), which allowed to deduce the following optimal conditions for the yield of SMT degradation, namely pH=6, Q_v=0.56 L/min and $[SMT]_0$= 11 mg/L. Under these optimal conditions, the SMT degradation yield experimentally obtained was y_{exp} = 98%, which should be related to that given by the model $\hat{y}$ = 96 %. The relative error between y_{exp} and $\hat{y}$ was below 2.8 %, validating the model, and hence the developed model describes accurately experimental data.

3.6. Biodegradability test

The biodegradability test was realized on solutions irradiated under the optimal values obtained by the CCD: pH=6, Q_v=0.56 L/min and $[SMT]_0$ = 11 mg/L. The biodegradability test was estimated by means of the BOD_5/COD ratio of the solutions irradiated during 5h and 8h. According to the table 3, it can be drawn that:

Accepted Manuscript

- The removal efficiency of SMT increased from 0 to 98 and 100 % when the irradiation time was increased from 0 to 5and 8h respectively.
- The COD abatement increased from 0 to 75% after 5h irradiation time; while an increase of the irradiation time from 5h to 8h did not show a significant impact on the COD abatement.
- The BOD_5/COD ratio increased from 0 initially to 0.20 after 5h of irradiation, showing that the biodegradability was enhanced even if the limit of biodegradability (0.4) was not achieved. However, further increase of the irradiation time, from 5 to 8h, induced a decrease of the BOD_5/COD ratio from 0.20 to 0, showing that the by-products formed after 8h of irradiation are not biodegradable. This decrease of the BOD_5/COD ratio may be also attributed to the adsorption of Zn^{2+} ions by activated sludge, which was reported to be the main mechanism of toxicity [49], while Wang et al [50] reported that Zn^{2+} ion is highly adsorbable on activated sludge. Indeed, the concentrations of Zn^{2+} ions after 8h of reaction time was estimated to 6 mg/L, while Lui et al [49] reported that the IC_{50} values of Zn^{2+} ions on biodegradation was 1.3 mg-Zn/ L.

Table 3

4. Conclusion

A response surface methodology based on CCD was successfully used for the study and the optimization of the removal efficiency of SMT by using UV/ZnO immobilized on glass plate. The application of the CCD with a second-order polynomial regression model satisfactorily interpreted the experimental data. It was shown that increasing the initial SMT concentration had negative effect on the removal efficiency. In addition, when the flow rates was increased

Accepted Manuscript

from 0.15 to 0.52 L/min, the SMT degradation increased from 74 % to 85%; while beyond 0.52 L/min flow rate, the yield of SMT degradation decreased from 85% to 81% for 0.68 L/min. The solution pH did not show significant impact on the removal efficiency of SMT in the studied interval. The use of CCD allowed the identification of the most significant interaction between parameters, shown to be between the pH and the flow rate. Analysis of the response surfaces and contour plots clearly indicated that the optimal values of solution pH, flow rate and initial SMT concentration were: 6, 0.56 L/min and 11 mg/L respectively. Under these optimal conditions, the SMT removal efficiency was 96 % and the BOD_5/COD ratio was increased from 0 to 0.20 after 5h of irradiation time.

Accepted Manuscript

References

[1] Babić S, Zrnčić M, Ljubas D, Ćurković L, Škorić I (2015) Photolytic and thin TiO_2 film assisted photocatalytic degradation of sulfamethazine in aqueous solution. Environ Sci Pollut Res 22:11372-11386

[2] Cesarino I, Simoes R.P, Lavarada F.C, Batagin-Neto A (2016) Electrochemical oxidation of sulfamethazine on a glassy carbon electrode modified with graphene and gold nano particles. Electrochimica Acta 192: 8-14

[3] Mansour D, Fourcade F, Bellakhal N, Dachraoui M, Hauchard D, Amrane A (2012) Biodegradability Improvement of Sulfamethazine Solutions by Means of an electro-Fenton Process. Water Air Soil Pollut 223:2023-2034

[4] Managaki S, Murata A, Takada T, Cach Tuyen B, Chiem N.H (2007) Distribution of macrolines, sulfonamides, and trimethoprim in tropical waters: ubiquitous occurrence of veterinary antibiotics in the Mekong Delta. Environ Sci Technol 41:8004-8010

[5] Yan C, Yang Y, Zhou J, Liu M, Nie M, Shi H, Gu L (2013) Antibiotics in the surface water of the Yangtze Estuary: occurrence, distribution and risk assessment. Environ Pollut 175:22-29

[6] Jiang L, Hu X, Yin D, Zhang H, Yu Z (2011) Occurrence, distribution and seasonal variation of antibiotics in the Huangpu River Shanghai, China. Chemosphere 82: 822-828

[7] Ledjeri A, Yahiaoui I, Kadji H, Aissani-Benissad F, Amrane A, Fourcade F (2017) Combination of the Electro/$Fe^{3+/}$peroxydisulfate (PDS) process with activated sludge culture for the degradation of sulfamethazine. Environ Toxicol Pharmacol 53:34-39

Accepted Manuscript

[8] Dinga H, Wua Y, Zoub B, Loub Q, Zhanga W, Zhong J, Lua L, Dai G (2016) Simultaneous removal and degradation characteristics of sulfonamide, tetracycline, and quinolone antibiotics by laccase-mediated oxidation coupled with soil adsorption. J Hazard Mater 307: 350-358

[9] Elmolla E.S, Chaudhuri M (2010) Photocatalytic degradation of amoxicillin, ampicillin and cloxacillin antibiotics in aqueous solution using UV/TiO_2 and UV/H_2O_2/TiO_2 photocatalysis. Desalination 252:46-52

[10] Sano T, Puzenat E, Guillard C, Geantet C, Matsuzawa S (2008) Degradation of C_2H_2 with modified-TiO_2 photocatalysts under visible light irradiation. J Mol Catal A-Chem 284:127-133

[11] Kitano M, Matsuoka M, Ueshima M, Anpo M (2007) Recent developments in titanium oxide-based photocatalysts. Appl Catal A-Gen 325:1-14

[12] Movahedi M, Mahjou A.R, Janitabar-Darzi S (2009) Photodegradation of congo red in aqueous solution on ZnO as an alternative Catalyst to TiO_2. J Iran Chem Soc 6:570-577

[13] Sapkal R.T, Shinde S.S, Mahadik M.A, Mohite V.S, Waghmode T.R, Govindwar S.P, Rajpure K.Y, Bhosale C.H (2012) Photoelectrocatalytic decolorization and degradation of textile effluent using ZnO thin films. J Photochem Photobiol B, Biol. 114:102-107

[14] Waghmode T.R, Kurade M. B, Sapkal R.T, Bhosale C. H, Jeon B.H, Govindwar S.P (2019) Sequential photocatalysis and biological treatment for the enhanced degradation of the persistent azo dye methyl red. J Hazard Mater 371:115–122

[15] Gao F, Yang Y, Wang T (2015) Preparation of porous TiO_2/Ag heterostructure films with enhanced photocatalytic activity. Chem Eng J 270:418-427

Accepted Manuscript

[16] Soltani R. D.C, Rezaee A, Khataee A.R, Safari M (2014) Photocatalytic process by immobilized carbon black/ZnO nanocomposite for dye removal from aqueous medium: Optimization by response surface methodology. J Ind Eng Chem 20:1861-1868

[17] Aber S, Khajeh R.T, Alireza Khataeeb A (2019) Application of immobilized ZnO nanoparticles for the photocatalytic regeneration of ultrasound pretreated-granular activated carbon. Ultrason Sonochem. https://doi.org/10.1016/j.ultsonch.2019.104685

[18] Vaiano V, Chianese L, Rizzo L, Iervolino G (2020) Visible light driven oxidation of arsenite to arsenate in aqueous solution using Cu-doped ZnO supported on polystyrene pellets. Catal Today. https://doi.org/10.1016/j.cattod.2020.01.011

[19] Boughelout A, Macaluso R, Kechouane M, Trari M (2020) Photocatalysis of rhodamine B and methyl orange degradation under solar light on ZnO and Cu_2O thin films. React Kinet Mech Catal 129:1115-1130

[20] Selvin S.S.P, Lee J, Kumar S, Radhika N, Merlin N.J, Lydia S (2017) Photocatalytic degradation of rhodamine B using cysteine capped ZnO/P(3HB-co-3HHx) fiber under UV and visible light irradiation. Reac Kinet Mech Cat 122:671-684

[21] Maučec D, Šuligoj A, Ristić A, Dražić G, Pintar A, Tušara N.N (2018) Titania versus zinc oxide nanoparticles on mesoporous silica supports as photocatalysts for removal of dyes from wastewater at neutral pH. Catal Today 310:32-41

[22] Han C, Andersen J, Likodimosb V, Falaras P, Linkugelc J, Dionysiou D.D (2014) The effect of solvent in the sol–gel synthesis of visible light-activated, sulfur-doped TiO_2 nanostructured porous films for water treatment. Catal Today 224:132-139

[23] Tseng T.K, Lin Y.S, Chen Y.J, Chu H (2010) A review of photocatalysts Prepared by Sol-Gel Method for VOCs Removal. Int J Mol Sci 11:2336-2361

[24] Chen H.S and Kumar R.V (2012) Sol–gel TiO_2 in self-organization process: growth, ripening and sintering. RSC Adv 2:2294–2301

Accepted Manuscript

[25] Li M, Lu B, Ke Q.F, Guo Y.J, Guo Y.P (2017) Synergetic effect between adsorption and photodegradation on nanostructured TiO_2/activated carbon fiber felt porous composites for toluene removal. J Hazard Mater 333:88-98

[26] Belver C, Bedia J, Rodriguez J.J (2017) Zr-doped TiO_2 supported on delaminated clay materials for solar photocatalytic treatment of emerging pollutants. J Hazard Mater 322:233-242

[27] Vicent M, Sánchez E, Moreno A, Rodrigo Moreno R (2012) Preparation of high solids content nano-titania suspensions to obtain spray-dried nanostructured powders for atmospheric plasma spraying. J Eur Cera Soc 32:185-194

[28] Yahia Cherif L, Yahiaoui I, Aissani-Benissad F, Madi K, Benmehdi N, Fourcade F, Amrane A (2014) Heat Attachment Method for the Immobilization of TiO_2 on Glass Plates: Application to Photodegradation of Basic Yellow Dye and Optimization of Operating Parameters, Using Response Surface Methodology. Ind Eng Chem Res 53:3813-3819

[29] Aissani T, Yahiaoui I, Boudrahem F, Ait Chikh S, Aissani-Benissad F, Amrane A (2018) The combination of photocatalysis process (UV/ TiO_2(P25) and UV/ZnO) with activated sludge culture for the degradation of sulfamethazine. Sep Sci Technol 35:1423-1424

[30] Yahiaoui I, Yahia Cherif L, Madi K, Aissani-Benissad F, Fourcade F, Amrane A (2018) The feasibility of combining an electrochemical treatment on a carbon felt electrode and a biological treatment for the degradation of tetracycline and tylosin-application of the experimental design methodology. Sep Sci Technol 53: 337-348

[31] Madi K, Yahiaoui I, Aissani-Benissad F, Vial C, Audonnet F, Lidia Favier L (2019) Basic red dye removal by coupling electrocoagulation process with biological treatment. Environ Eng Manag J. 18: 563-573

Accepted Manuscript

[32] Dibene K, Yahiaoui I, Aitali S, Khenniche L, Amrane A, Aissani-Benissad F (2019) Central composite design applied to paracetamol degradation by heat-activated peroxydisulfate oxidation process and its relevance as a pretreatment prior to a biological treatment. https://doi.org/10.1080/09593330.2019.1649308

[33] Yahiaoui I, Aissani-Benissad F, Fourcade F, Abdeltif Amrane A (2015) Removal of a mixture tetracycline-tylosin from water based on anodic oxidation on a glassy carbon electrode coupled to activated sludge. Environ Technol 36:1837-1846

[34] Ferrag-Siagh F, Fourcade F, Soutrel I, Aït-Amar H, Djelala H, Amrane A, (2013) Tetracycline degradation and mineralization by the coupling of an electro-Fenton pretreatment and a biological process. J Chem Technol Biotechnol. 88:1380-1386

[35] Yahiaoui I, Aissani-Benissad F, Ait amar H (2010) Optimization of silver cementation yield in fixed bed reactor using factorial design and central composite design. Can J Chem Eng 6:1099-1106

[36] Yahiaoui I, Aissani-Benissad F, Fourcade F, Amrane, A (2012) Response surface methodology for the optimization of the electrochemical degradation of phenol on Pb/PbO_2 electrode. Environ Prog Sustain Energy 31:515-523

[37] Yahiaoui I, Belattaf A, Aissani-Benissad F, Yahia Cherif L (2011) Full factorial design applied to a biosorption of lead (II) ions from aqueous solution using a brewer's yeast (Saccharomyces cerevisiae). J Chem Eng Data 56:3999-4005

[38] Kosera V.S, Cruz T.M, Chaves E.S, Tiburtius E.R.L (2017) Triclosan degradation by heterogeneous photocatalysis using ZnO immobilized in biopolymer as catalyst. J Photochem Photobiol A Chem 344: 184-191

Accepted Manuscript

[39] Kosmulski M (2009) Compilation of PZC and IEP of sparingly soluble metal oxides and hydroxides from literature. Adv Colloid Interface Sci 152:14–25

[40] Benhebal H, Chaib M, Salmon T, Geens J, Leonard A , Lambert S.D, Crine M , Heinrichs B (2013) Photocatalytic degradation of phenol and benzoic acid using zinc oxide powders prepared by the sol–gel process. Alex Eng J 52: 517–523

[41] Khenniche L, Favierc L, Bouzazac A, Fourcade F, Aissani F, Amrane A (2015) Photocatalytic degradation of bezacryl yellow in batch reactors-feasibility of the combination of photocatalysis and a biological treatment. Environ Technol 36:1-10

[42] Andronic L, Enesca L, Vladuta A, Duta C.A (2009) Photocatalytic activity of cadmium doped TiO_2 films for photocatalytic degradation of dyes. Chem Eng J 152:64-71

[43] Lou W, Kane A, Wolbert D, Rtimi S, Assadi A.A (2017) Study of a photocatalytic process for removal of antibiotics from wastewater in a falling film photoreactor: Scavenger study and process intensification feasibility. Chem Eng Process: Process Intensification 122:213-221

[44] Zayani G, Bousselmi L, Mhenni F, Ghrabi, A (2009) Solar photocatalytic degradation of commercial textile azo dyes: Performance of pilot plant scale thin film fixed-bed reactor. Desalination 246:344-352

[45] Daneshvar N, Salarib D, Khataeea A.R (2004) Photocatalytic degradation of azo dye acid red 14 in water on ZnO as an alternative catalyst to TiO_2. J Photochem Photobiol A 162:317–322

[46] Zhang L, Cheng H, Zong R, Zhu Y (2009) Photocorrosion suppression of ZnO nanoparticles via hybridization with graphite-like carbon and enhanced photocatalytic activity. J Phys Chem C 113:2368-2374

Accepted Manuscript

[47] Boudrahem F, Aissani-Benissad F, Soualah A (2014) Removal of basic yellow dye from aqueous solutions by sorption onto reed as an adsorbent. Desalination Water Treat 54:1727-1734

[48] Sakthivel S, Neppolian B, Shankar M.V, Arabindoo B, Palanichamy M, Murugesan V (2003) Solar photocatalytic degradation of azo dye: comparison of photocatalytic efficiency of ZnO and TiO_2. Sol Energy Mater Sol Cells 77:65-82

[49] Liu G, Wang D, Wang J, Mendoza C (2011) Effect of ZnO particles on activated sludge: Role of particle dissolution. Sci Total Environ 409:2852–2857

[50] Wang J, Huang C.P, Allen H.E (2003) Modeling heavy metal uptake by sludge particulates in the presence of dissolved organic matter. Water Res 37:4835-4842

Accepted Manuscript

Figure captions

Figure 1: The effect of the amount of ZnO immobilized on glass plate. Conditions: pH = 6, T = 25°C, , time = 300 min and Q_v=0.52 L/min

Figure 2: The removal efficiency of SMT within the successive six cycles. Conditions: $[SMT]_0$ = 50mgL^{-1}, pH = 6, T = 25°C , Q_v=0.52 L/min, , time = 300 min and 0.16 g of ZnO immobilized on glass plate.

Figure 3: Effect of initial concentration of sulfamethazine (SMT) on the photocatalytic degradation process. Conditions: 0.16g of ZnO, pH = 6, Q_v=0.52 L/min, and T = 25°C.

Figure 4: Effect of flow rate (Q_v) on photodegradation efficiency of SMT. Conditions: $[SMT]_0$ = 50 mg/L, T=25°C, time = 300 min and 0.16g of ZnO immobilized on glass plate .

Figure 5: Effect of pH solution on photodegradation efficiency of SMT. Conditions: $[SMT]_0$= 50 mg/L, Q_v=0.52 L/min, T = 25°C and 0.16 g of ZnO immobilized on glass plate.

Figure 6: Experimental data, first-order kinetic model, second-order kinetic model, and Langmuire–Hinshelwood model for photocatalytic degradation of SMT by ZnO Immobilized on glass plate. Experimental conditions: 0.16g of ZnO, pH = 6, Q_V = 0.52L/min, and T = 25°C

Accepted Manuscript

Tables

Table 1. The values of film thickness of the liquid at the different flow rates tested

Q_v (L/min)	0.15	0.371	0.521	0.681
Film thickness(mm)	0.19	0.34	0.43	0.51

Accepted Manuscript

Table 2. Kinetic constants predicted by non-linear method for the photocatalytic degradation of SMT by ZnO immobilized on glass plate.

$[SMT]_0$ (mg/l)	First order model		Second-order model		L-H Kinetic model		
	k_1(min^{-1})	D (%)	k_2(l/mg min)	D (%)	k(min^{-1})	K	D (%)
10	0.012 ±1.8410^{-3}	0.085	0.002 ±3.41 10^{-4}	5.2	0.34 ±8.35 10^{-2}	0.067 ±3.05 10^{-2}	0.023
50	0.006 ±5.910^{-4}	0.11	0.0001 ±1.36 10^{-5}	2.5	0.26 ±8.9 10^{-4}	0.64 ± 7.9 10^{-3}	0.34
100	0.005 ±1.110^{-3}	0.2	5.7.10^{-5} ±1.03 10^{-5}	0.3	6.18 ±1.4 10^{-2}	0.00085 ± 2.68 10^{-5}	0.56

Accepted Manuscript

Table 3. Removal efficiency of SMT, COD abatement and biodegradability tests of solutions pretreated by the photocatalytic process in the following conditions: pH = 6, T = 25°C and Q_v= 0.56 L/min.

		Irradiation time (h)		
$[SMT]_0$ (mg/L)		*0*	*5*	*8*
11	Removal efficiency of SMT (%)	*0*	*98*	*100*
	COD abatement (%)	*0*	*75*	*75*
	BOD_5/COD	*0*	*0.20*	*0*

Accepted Manuscript

Figures

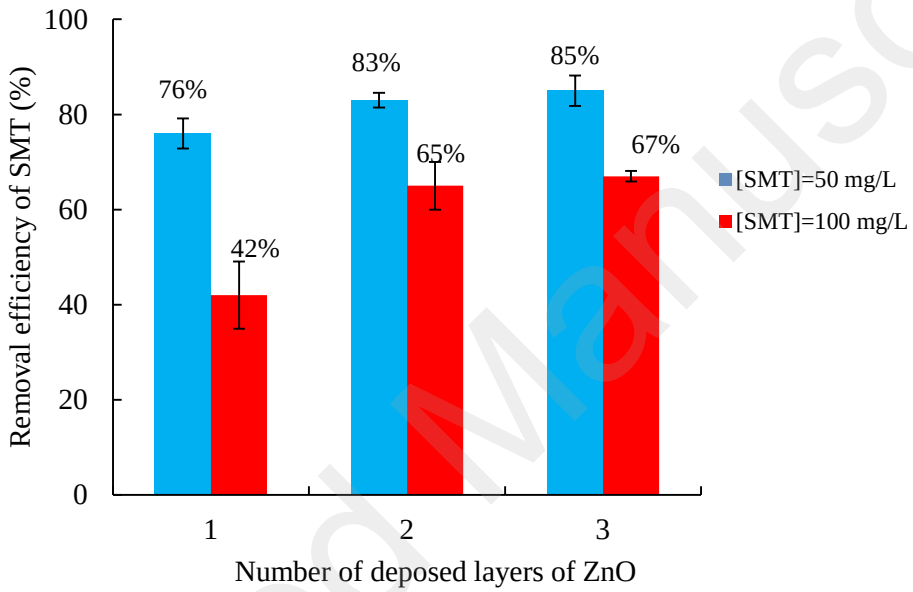

Fig. 1

Accepted Manuscript

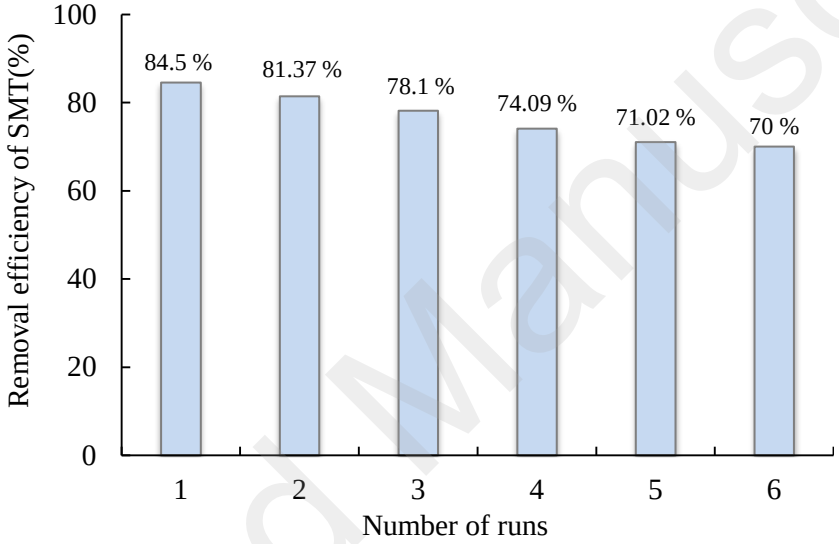

Fig. 2

Accepted Manuscript

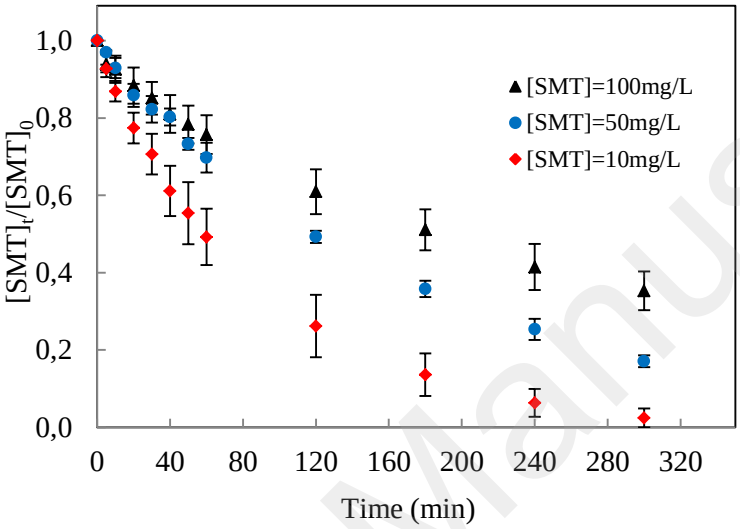

Fig.3

Accepted Manuscript

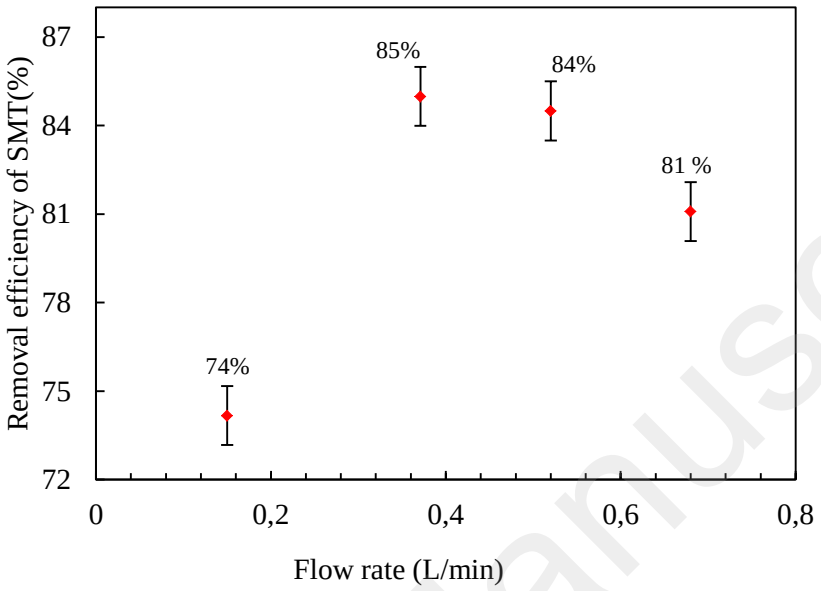

Fig.4

Accepted Manuscript

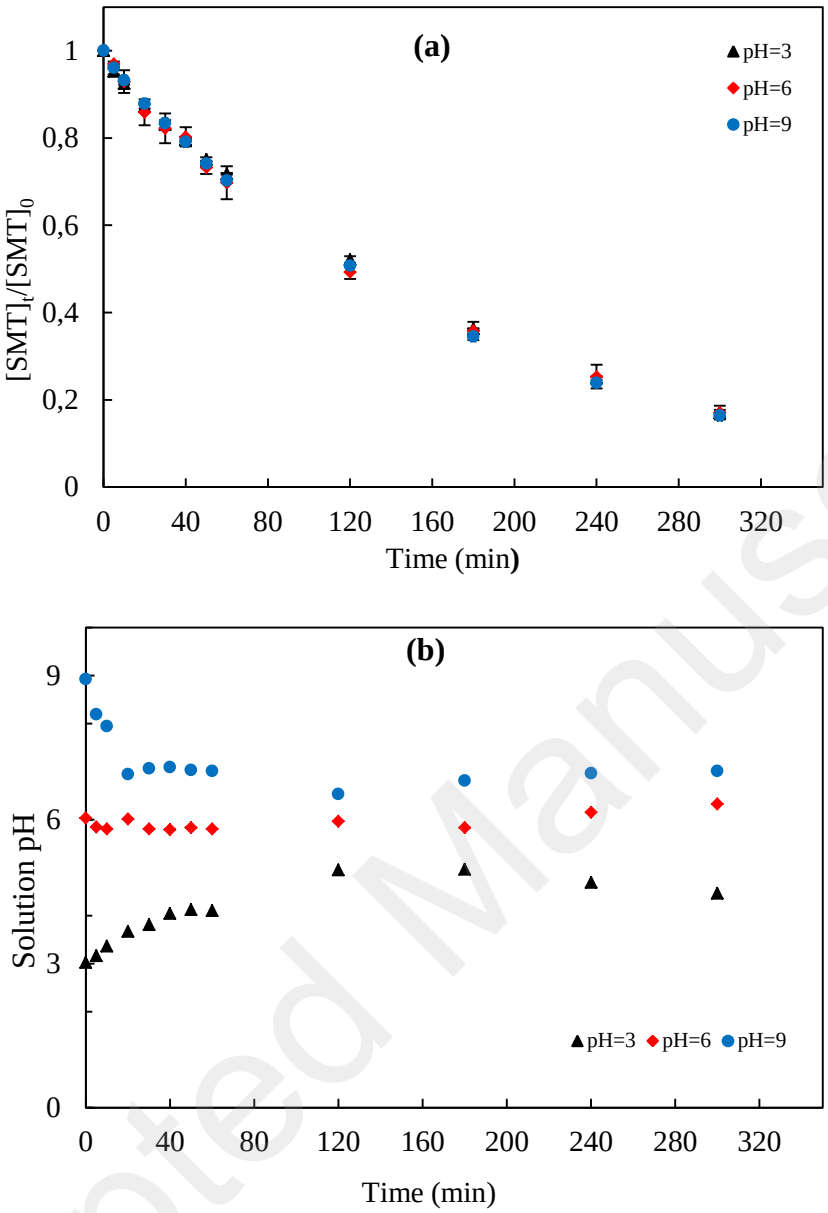

Fig.5

Accepted Manuscript

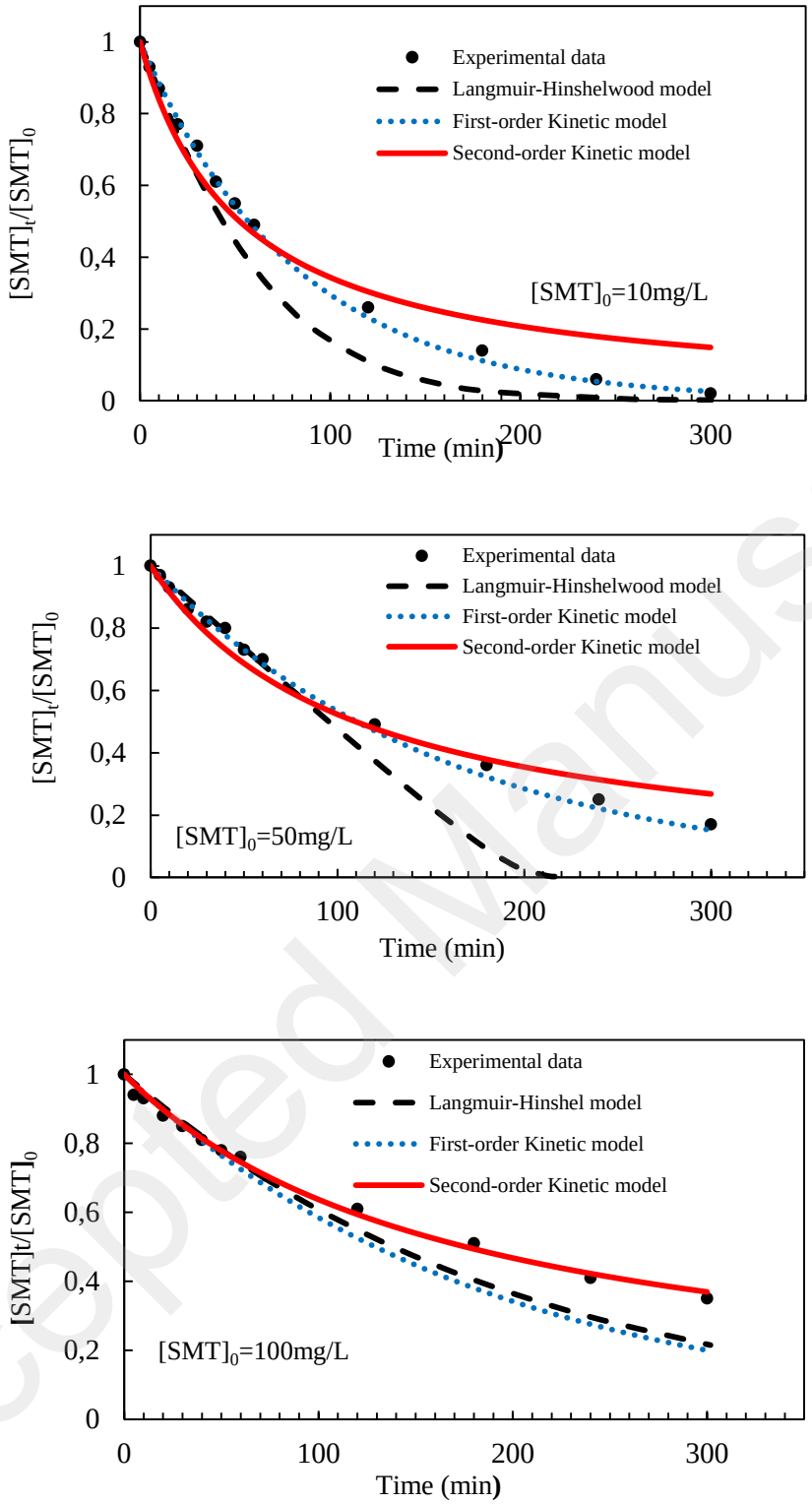

Fig.6

Accepted Manuscript